control strategies typical for manipulation[29]. Second, in action observation, as in action, gaze was rarely directed towards the moving hand, as might be expected if hand motion were being visually analysed[30]. Third, when subjects observed blocks moving without hand involvement, the gaze pattern differed from that engaged in action and action observation by being reactively coupled to the events. This result matches findings showing that the part of the motor representation to which the mirror system belongs is activated only when the observer views an object-oriented goal-directed task and not when the observer views its components[1,2,18]. □

Methods

Subjects

Nine women and seven men aged from 19 to 30 years participated after providing written informed consent. All subjects were healthy, were right-handed, had normal vision and were naive as to the purpose of the experiment.

Block stacking task

The wooden blocks were located on a 19-cm wide work surface (Fig. 1a) centred 39 cm in front of the eyes and 8 cm below eye level. Eight subjects both performed the block stacking task and observed an actor performing the task who sat across from them. In both tasks, nine stacking trials performed at a preferred rate were followed by nine trials performed at a faster rate. In each block of nine trials, six were performed with an obstacle in the form of a vertically oriented block located in the centre of the workspace. These trials were interspersed among three trials without an obstacle. We focused our analysis on the latter trials. Each stacking trial was followed by an unstacking trial and between all trials subjects moved the hand to a parking position located 29 cm below and 4 cm to the right of the work surface.

Eight additional subjects observed the same block stacking task performed at the preferred rate by the same actor who was hidden from view. In this condition, the actor was positioned below the work surface and reached up to grasp tabs attached to the back surface of each block. The actor wore black gloves and a black outfit so as not to be visible against the black drape positioned behind the work surface in all conditions. Subjects were given no instructions on where to look in any of the three block stacking tasks.

Gaze position of the right eye in the plane in which the blocks were moved was recorded using an infrared eye tracking system and the position of the tip of the right index finger of the subject or actor were recorded with miniature electromagnetic sensors attached to the nail. A haptic calibration procedure was used to estimate the position on the distal pad of the index finger when in contact with a block. A bite bar was used to stabilize the head. The apparatus, calibration procedures and the accuracy and resolution of all measures have been described in detail elsewhere[22].

Data processing

To preserve phase information when combining data from different trials for plotting, we first segmented each trial into seven contiguous phases based on when the index finger crossed a vertical line located at $x = 6$ (see Fig. 1a); the start and end of hand movement defined the beginning and end of the first and last phases, respectively. We then normalized the time base of each phase to the median duration of that phase. We defined trial duration, for use in statistical analysis, as the time from the end of the first phase to the start of the last. We detected the occurrences of saccades based on a filter applied to the gaze position signals combined with a threshold criterion as described[22].

Received 6 May; accepted 13 June 2003; doi:10.1038/nature01861.

---

1. Gallese, V., Fadiga, L., Fogassi, L. & Rizzolatti, G. Action recognition in the premotor cortex. *Brain* **119,** 593–609 (1996).
2. Rizzolatti, G., Fadiga, L., Gallese, V. & Fogassi, L. Premotor cortex and the recognition of motor actions. *Brain Res. Cogn. Brain Res.* **3,** 131–141 (1996).
3. Iacoboni, M. *et al.* Cortical mechanisms of human imitation. *Science* **286,** 2526–2528 (1999).
4. Rizzolatti, G., Fogassi, L. & Gallese, V. Neurophysiological mechanisms underlying the understanding and imitation of action. *Nature Rev. Neurosci.* **2,** 661–670 (2001).
5. di Pellegrino, G., Fadiga, L., Fogassi, L., Gallese, V. & Rizzolatti, G. Understanding motor events: a neurophysiological study. *Exp. Brain Res.* **91,** 176–180 (1992).
6. Fadiga, L., Fogassi, L., Pavesi, G. & Rizzolatti, G. Motor facilitation during action observation: a magnetic stimulation study. *J. Neurophysiol.* **73,** 2608–2611 (1995).
7. Hari, R. *et al.* Activation of human primary motor cortex during action observation: a neuromagnetic study. *Proc. Natl Acad. Sci. USA* **95,** 15061–15065 (1998).
8. Nishitani, N. & Hari, R. Temporal dynamics of cortical representation for action. *Proc. Natl Acad. Sci. USA* **97,** 913–918 (2000).
9. Strafella, A. P. & Paus, T. Modulation of cortical excitability during action observation: a transcranial magnetic stimulation study. *NeuroReport* **11,** 2289–2292 (2000).
10. Gangitano, M., Mottaghy, F. M. & Pascual-Leone, A. Phase-specific modulation of cortical motor output during movement observation. *NeuroReport* **12,** 1489–1492 (2001).
11. Umiltà, M. A. *et al.* I know what you are doing: a neurophysiological study. *Neuron* **31,** 155–165 (2001).
12. Avikainen, S., Forss, N. & Hari, R. Modulated activation of the human SI and SII cortices during observation of hand actions. *NeuroImage* **15,** 640–646 (2002).
13. Kohler, E. *et al.* Hearing sounds, understanding actions: action representation in mirror neurons. *Science* **297,** 846–848 (2002).
14. Grafton, S. T., Arbib, M. A., Fadiga, L. & Rizzolatti, G. Localization of grasp representations in humans by positron emission tomography. 2. Observation compared with imagination. *Exp. Brain Res.* **112,** 103–111 (1996).
15. Rizzolatti, G. *et al.* Localization of grasp representations in humans by PET: 1. Observation versus execution. *Exp. Brain Res.* **111,** 246–252 (1996).
16. Decety, J. *et al.* Brain activity during observation of actions. Influence of action content and subject's strategy. *Brain* **120,** 1763–1777 (1997).
17. Iacoboni, M. *et al.* Reafferent copies of imitated actions in the right superior temporal cortex. *Proc. Natl Acad. Sci. USA* **98,** 13995–13999 (2001).
18. Koski, L. *et al.* Modulation of motor and premotor activity during imitation of target-directed actions. *Cereb. Cortex* **12,** 847–855 (2002).
19. Land, M. F. & Furneaux, S. The knowledge base of the oculomotor system. *Phil. Trans. R. Soc. Lond. Biol.* **352,** 1231–1239 (1997).
20. Land, M., Mennie, N. & Rusted, J. The roles of vision and eye movements in the control of activities of daily living. *Perception* **28,** 1311–1328 (1999).
21. Land, M. F. & McLeod, P. From eye movements to actions: how batsmen hit the ball. *Nature Neurosci.* **3,** 1340–1345 (2000).
22. Johansson, R. S., Westling, G., Bäckström, A. & Flanagan, J. R. Eye-hand coordination in object manipulation. *J. Neurosci.* **21,** 6917–6932 (2001).
23. Ballard, D. H., Hayhoe, M. M., Li, F. & Whitehead, S. D. Hand-eye coordination during sequential tasks. *Phil. Trans. R. Soc. Lond. Biol.* **337,** 331–338 (1992).
24. Ballard, D. H., Hayhoe, M. M. & Pelz, J. B. Memory representations in natural tasks. *J. Cogn. Neurosci.* **7,** 66–80 (1995).
25. Becker, W., (ed. Carpenter, R. H. S.)) 95–137 (Macmillan, London, 1991).
26. Rizzolatti, G., Fadiga, L., Fogassi, L. & Gallese, V. Resonance behaviors and mirror neurons. *Arch. Ital. Biol.* **137,** 85–100 (1999).
27. Perrett, D. I. *et al.* Frameworks of analysis for the neural representation of animate objects and actions. *J. Exp. Biol.* **6,** 87–113 (1989).
28. Allison, T., Puce, A. & McCarthy, G. Social perception from visual cues: role of the STS region. *Trends Cogn. Sci.* **4,** 267–278 (2000).
29. Johansson, R. S. & Cole, K. J. Sensory-motor coordination during grasping and manipulative actions. *Curr. Opin. Neurobiol.* **2,** 815–823 (1992).
30. Mataric, M. J. & Pomplun, M. Fixation behavior in observation and imitation of human movement. *Brain Res. Cogn. Brain Res.* **7,** 191–202 (1998).

Acknowledgements We thank G. Westling and A. Bäckström for engineering and software support. This study was supported by the Canadian Institutes of Health Research, the Swedish Medical Research Council, the Göran Gustafsson Foundation for Research in Natural Sciences and Medicine, and the 5th Framework Program of European Union.

Competing interests statement The authors declare that they have no competing financial interests.

Correspondence and requests for materials should be addressed to R.F. (flanagan@psyc.queensu.ca).

Prediction of auditory spatial acuity from neural images on the owl's auditory space map

Avinash D. S. Bala, Matthew. W. Spitzer & Terry T. Takahashi

Institute of Neuroscience, University of Oregon, Eugene, Oregon 97403, USA

The owl can discriminate changes in the location of sound sources as small as 3° and can aim its head to within 2° of a source[1,2]. A typical neuron in its midbrain space map has a spatial receptive field that spans 40°—a width that is many times the behavioural threshold[3]. Here we have quantitatively examined the relationship between neuronal activity and perceptual acuity in the auditory space map in the barn owl midbrain. By analysing changes in firing rate resulting from small changes of stimulus azimuth, we show that most neurons can reliably signal changes in source location that are smaller than the behavioural threshold. Each source is represented in the space map by a focus of activity in a population of neurons. Displacement of the source causes the pattern of activity in this population to change. We show that this change predicts the owl's ability to detect a change in source location.

We measured spatial discrimination behaviour by using the pupillary dilation response (PDR)[2]. The barn owl's pupil dilates on presentation of a sound and habituates on repeated presentation of the same stimulus. When the stimulus is changed by presenting the same sound from a different location, the PDR recovers (Fig. 1a). We habituated the PDR by repeated presentation of a broadband noise (Fig. 1a, black marker) from a source at azimuth $x°$, and looked for recovery on presenting the identical noise burst from another source at azimuth $x° + \Delta x°$. Discrimination was quantified by expressing the difference in the PDR magnitudes evoked by habituating stimuli (from azimuth $-3°$; Fig. 1a, broken lines) and test stimuli (from azimuth 3°; Fig. 1a, unbroken lines) in units of their combined s.d. A non-parametric index of discrimination, standard separation[4], D, was computed as follows:

$$D = \left|(\mu_x - \mu_{x+\Delta x})/\sqrt{(\sigma_x \sigma_{x+\Delta x})}\right| \qquad (1)$$

where μ_x and $\mu_{x+\Delta x}$ refer to the mean magnitudes of the PDR to habituating and test stimuli, and σ_x and $\sigma_{x+\Delta x}$ are the respective s.d. D does not saturate, unlike another non-parametric measure of discrimination, proportion correct, $p(c)$, which allowed us to assess the relationship between behavioural and neuronal discrimination above threshold.

In Fig. 1b, behavioural discrimination ($D_{\mathrm{behaviour}}$) is plotted against the angular separation ($\Delta x°$) of the two sources for three birds. The minimum audible angle (MAA) was defined as the smallest angular separation giving rise to $D_{\mathrm{behaviour}} \geq 0.8$, which corresponds to 0.75 $p(c)$. The MAA was 3° for all three birds tested. Identical MAAs were observed according to a t-test ($P < 0.01$). This MAA is within the range of head-aim errors (1.7° to 4°) in a head-pointing task[1], another measure of spatial acuity. The psychometric functions shown in Fig. 1b can also be thought of as "generalization gradients"[5]—that is, functions that describe the recovery of a habituated response as test and habituating stimuli become more dissimilar. Space-specific neurons (SSNs) in the owl midbrain, which constitute the space map, respond to source displacement by changing their firing rate. This change in firing rate provides a basis for recovery of the habituated response, even though SSNs themselves do not habituate. We investigated the relationship between the behavioural generalization gradient described above and the rate of change of neuronal activity in the space map.

The change in the neuronal image of the space map caused by displacing the source from x to $x + \Delta x$ was assessed in SSNs tuned to frontal space ($-20°$ to $+20°$ azimuth; $-20°$ to $+20°$ elevation; Fig. 2a). The spatial receptive field (SRF) of isolated SSNs was first charted coarsely using broadband noise presented in virtual auditory space (VAS[6]; Fig. 2b). A cross-section through the centre of the SRF was then sampled in 1° increments (Fig. 2b, white line, and 2c, black line). Neuronal discrimination (D_{neuron}) was then computed by assessing the change in firing rates evoked by sources at each pair of azimuthal locations separated by $\Delta x°$ using equation (1). In the neuronal case, μ_x and $\mu_{x+\Delta x}$ refer to the mean firing rates at two

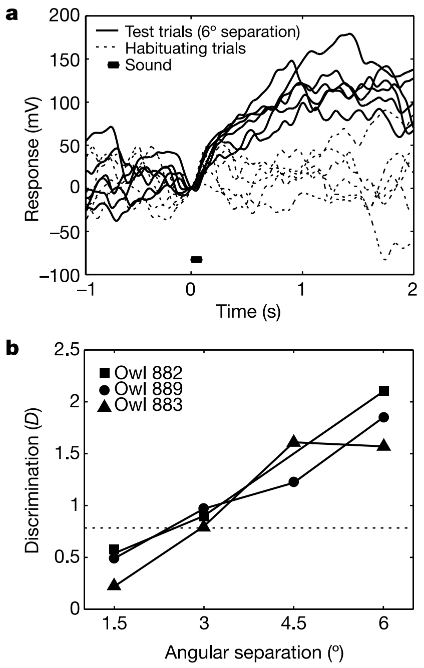

Figure 1 Behavioural discrimination of azimuthal source separation. **a**, Voltage traces representing pupillary responses to test (unbroken lines) and habituating (broken lines) stimuli from a single session (owl 883). Sources in this session were separated by 6° in azimuth. **b**, Behavioural discrimination measured in three subjects. Horizontal line represents the arbitrary discrimination threshold ($D = 0.8$).

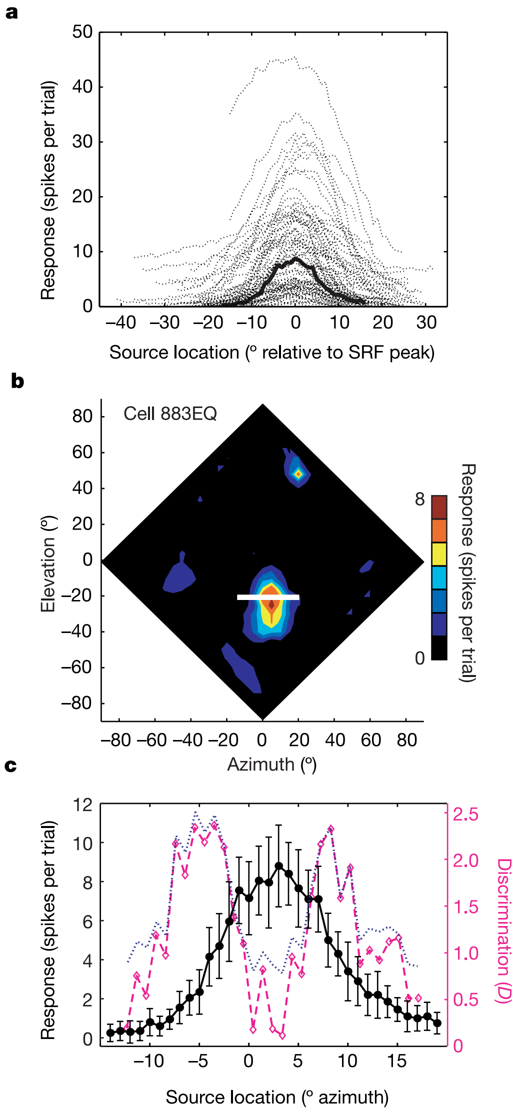

Figure 2 Neuronal discrimination. **a**, Azimuth tuning functions of 83 neurons, aligned such that the peaks are located at 0° azimuth. Unit 883EQ is indicated by the bold line. **b**, SRF of a typical space-map neuron from owl 883. White line represents the azimuthal cross-section assayed at a resolution of 1°. **c**, Neuronal responses are shown in black (mean ± s.d.). Discrimination performance (magenta) was computed for source pairs separated by 3°. The broken blue line depicts the output of a discrimination model (see text).

locations separated by $\Delta x°$, and σ_x and $\sigma_{x+\Delta x}$ refer to the respective s.d. Because sources at x and $x + \Delta x$ will affect neurons differently depending on the locations of their SRF, this method estimates the change in activity across a population of neurons.

Magenta symbols in Fig. 2c represent the D_{neuron} values for all pairs of sources separated by $\Delta x = 3°$. Note that discrimination performance, differs across the extent of the SRF, because it is related to both the change in response and the variance across a 3° separation. Figure 2c shows that this cell could signal 3° changes in source azimuth at suprathreshold levels ($D_{\text{neuron}} \geq 0.8$) at many locations along its SRF. At best, this cell discriminated a 3° separation at a performance of $D_{\text{neuron}} = 2.36$. More than 90% of the units sampled were similar to this example, in that the maximum discrimination performance at a given value of Δx exceeded the owl's behavioural performance. This indicates that the owl does not need to pool responses across coarsely tuned neurons to improve neuronal discrimination[7–10]. The finding that maximal neuronal acuity exceeds behavioural acuity is inconsistent with the hypothesis that behavioural thresholds are determined by thresholds of the most sensitive neurons[11,12] and is similar to the findings of studies in cerebral cortex[13–17].

As the source separation is increased, neuronal discrimination performance improves. We plotted D_{neuron} values, derived from all 83 neurons, as a function of azimuthal separation (Fig. 3, magenta diamonds). The mean of all of the D_{neuron} values (magenta line), which represents the average change in space-map activity evoked by source displacement, is statistically indistinguishable from the mean behavioural performance (Figs 3 and 4, broken black line; Mann–Whitney U-test; $P > 0.05$). This finding suggests that recovery from habituation or, equivalently, behavioural discrimination performance, is mediated by the change of population activity in the space map.

How could the change in population activity drive the PDR? Although it is premature to propose specific circuitry, we propose a model with the following properties. First, SSNs project to a layer of neurons that habituate to repeated presentation of a stimulus[18], and habituation occurs independently in each neuron[19,20]. Because firing rates vary within as well as across neurons (Fig. 2a, b), the degree of depression for each input must depend on the accumulated firing rate and variance of the afferent SSN in response to repeated presentation of the habituating stimulus. This is accomplished by normalizing the output of each SSN by the s.d. of these responses. Although the response to the habituating stimuli (R_{HS}) declines, the response (R) to stimuli presented from other locations continues (equation (2), Methods).

Second, outputs from the habituating neurons project to an integrator that ultimately controls the magnitude of the PDR. The integrated output is graded, as is the PDR itself, and is directly proportional to behavioural performance. On averaging or scaling by the number of participating neurons (ref. 21 and equation (3), Methods), the integrator output matches behavioural performance (Fig. 4, blue line). Conceptually, this model resembles the proposed novelty detectors in the amygdala[22] and would constitute a part of the hippocampal component of the complementary learning systems model[23]. The performance of this model, if the space map were composed solely of neurons identical to unit 883EQ, approximates its D_{neuron} values (Fig. 2c, broken blue line). Figure 4 shows the results generated with inputs from all 83 neurons (broken blue line), which yields a good match with behaviour.

Discrimination values derived from single neurons (Fig. 3, magenta diamonds) can be combined in many other ways[16,24–26], all of which improve performance. Because the discrimination performance of single neurons can exceed behavioural performance, such pooling schemes yield values that far exceed behavioural performance: optimal pooling[24] of individual D_{neuron} values yields $D = 69.23$ for a 3° separation, whereas $D_{\text{behaviour}} = 0.89$. Similarly, discrimination values derived from summing spike rates across all neurons in our sample, which reduces variance, vastly exceed behaviour. Thus, the amount of information present in space-map neurons far exceeds that used for this behaviour, and the owl combines these D_{neuron} values in a non-optimal manner[25].

If behaviour could be performed better by single neurons, why would the owl bother with a population representation? Representation of sensory stimuli in populations has inherent advantages, such as elimination of dimensional ambiguity. First, the firing rates of single space-map neurons change in response to alterations not only in stimulus location but also in sound intensity, and such changes produce unambiguous alterations in the collective representation on the space map. Second, a distributed representation is insensitive to the loss of a few constituent neurons. Third, it is conceivable that the information in the space map could be combined in more optimal ways for other tasks, such as sound localization in a multisource environment. Last, our analysis assumes that our discrimination data represent several independent observations of the same stimulus change, and that responses across neurons are uncorrelated. Local connections among neurons exist

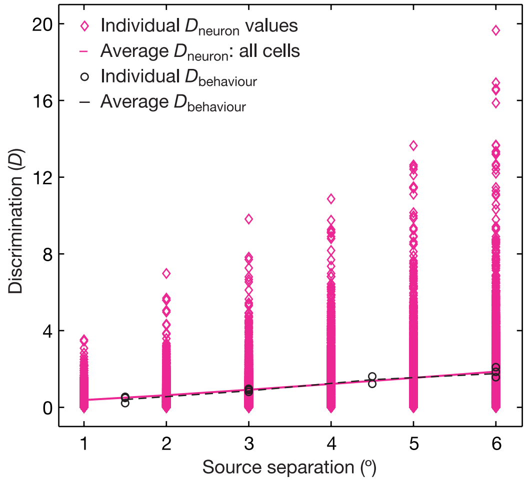

Figure 3 Average neuronal discrimination approximates behavioural performance. At all separations tested, individual neuronal discrimination values (magenta diamonds) can equal or exceed behavioural performance (black circles and line).

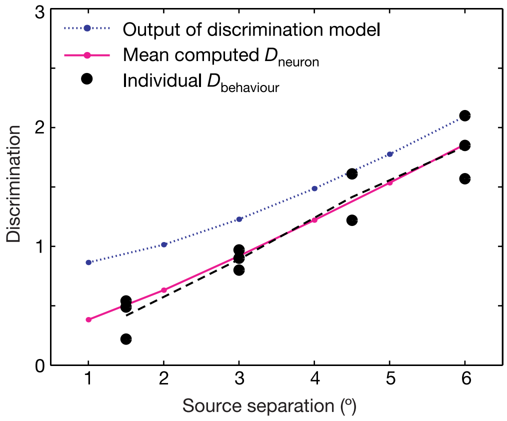

Figure 4 Neuronal computation of spatial discrimination. Discrimination performance by the habituation-based discrimination model (dotted blue line) yields results that approximate behavioural performance.

throughout the auditory system in the owl[27], which could lead to some degree of correlation among the responses of space-map neurons. Such correlations would significantly degrade the efficacy of pooling across neurons[28].

The change in the neural image, quantified here by measuring changes in the response of space-map neurons caused by azimuthal translocation of a sound source, is an internal 'decision variable' that the PDR circuitry uses to determine the magnitude of a response. It can also function as the decision variable in operant models, such as rating and two-interval forced choice tasks, in which the stimulus at the moment must be compared with a stored representation[18,22,23,29,30] to generate a response. □

Methods

Owls

Subjects were captive bred adult barn owls of either sex. We used three owls for behavioural assessment (owls 882, 883, 889) and three for neuronal recordings (owls 883, 719, 896). Experimental procedures were approved by the Institutional Animal Care and Use Committee, University of Oregon.

Behaviour

Spatial discrimination behaviour was assessed in a head-fixed preparation by the PDR[2]. The acoustically evoked PDR was habituated by repeated presentation of sounds from a speaker at a single location. Sounds were 100-ms frozen bursts of noise (3–11 kHz) with 5-ms on and off ramps, presented at 52 dBA (A-weighted sound pressure level). This range encompassed frequencies relevant for sound localization in the owl[1]. After habituation (50 sounds, presented once every 12 ± 2 s), sounds were presented from another location that symmetrically straddled the midline. Test stimuli were presented once every 20 trials, resulting in one measurement of the PDR to test stimuli and one measurement of PDR to the habituating stimuli every 4–6 min.

Pupillary dilation was monitored using an infrared pupillometer, which transduced dilation into voltage. The magnitude of the PDR was measured by integrating the output voltage of the pupillometer over 2 s after stimulus onset. The magnitude of the PDR in response to sounds presented from the habituating location—specifically, the magnitude of response of a few randomly selected trials, designated as 'catch trials'—could be then compared with the magnitude of the PDR to sounds from the test location. Typically, 5–7 measurements of each spatial separation were made in a single session lasting 50–70 min. Results were pooled across 4–5 sessions (20–25 observations per separation) to derive discrimination values (see text).

Neurophysiology

Responses of isolated space-specific neurons were recorded in anaesthetized owls. Units could be localized to the exterior nucleus of the inferior colliculus (ICx) on the basis of their response characteristics and location relative to the central nucleus of the inferior colliculus (IC core). Anaesthesia was induced with ketamine and valium, and maintained for the course of the experiment (10–12 h) with nitrous oxide supplemented by isofluorane as needed. We determined each neuron's SRF at a resolution of 10° by presenting broadband bursts (2–11 kHz) from 292 virtual locations.

VAS stimuli were generated by using location-specific filters derived from the head-related transfer functions (HRTFs) of each owl. HRTFs were measured[6] at a resolution of 5° across the frontal hemisphere (619 locations) and at a resolution of 1° in selected regions of frontal space (245 locations). The sound pressure of VAS stimuli was 50 dBA, which is very close to the level at which behaviour was measured (52 dBA), and was typically 25–30 dB above neuronal threshold. The firing rate of most of these neurons at their best location saturated at 25 dB above threshold. Azimuthal receptive fields were assessed at a resolution of 1° at one of five different elevations: 0°, ±10° and ±20°. Note that the SRFs of space-specific neurons are typically elongated in elevation, and the peak responding area almost always intersected one of the five elevations at which azimuthal discrimination was measured at higher resolution.

Spike counts were measured in a window corresponding to the duration of the sound, delayed by the neuronal response latency. Sounds were presented 20 times from each location, yielding a sample size large enough to assess response variance. For neurons in which we were unable to assess the whole width of the SRF (see the highest responding neuron, Fig. 2c), discrimination was assessed only on the side for which the whole slope, from foot to peak, was sampled. The partially sampled half was not included for analysis.

Neuronal computational model

The output of each space-map neuron is normalized by passage through a linear transformation function, causing the spike rate to be scaled down. This normalized output is then projected to a layer of habituating neurons, where the responses to sound from the habituating stimuli (R_{HS}) decline on repeated presentation. This results in a habituation gradient, where the output of the habituating cell declines to presentation of sounds from the habituating location, but declines less as the test source moves further from the habituating location:

$$\mathrm{Output}_{\mathrm{habituated}} = R - \mathrm{mean}(R_{\mathrm{HS}}) \quad (2)$$

The habituated output yields two sets of values, for test and catch trials, from which discrimination can be computed as in equation (1). Note that when responses are normalized to the s.d. of R_{HS}, the habituated output equals the z-score, which is similar to the computed D (Fig. 3, blue line). The output of each neuron in the habituating layer is summed and averaged[21]:

$$D_{\mathrm{pop}} = (\Sigma_1^n D_{\mathrm{neuron}})/n \quad (3)$$

The resultant output yields a close match with behaviour (Fig. 4, blue line).

Received 27 December 2002; accepted 13 June 2003; doi:10.1038/nature01835.

---

1. Knudsen, E. I., Blasdel, G. G. & Konishi, M. Mechanisms of sound localization in the barn owl (*Tyto alba*). *J. Comp. Physiol. A* **133,** 13–21 (1979).
2. Bala, A. D. & Takahashi, T. T. Pupillary dilation response as an indicator of auditory discrimination in the barn owl. *J. Comp. Physiol. A* **186,** 425–434 (2000).
3. Knudsen, E. I., Konishi, M. & Pettigrew, J. D. Receptive fields of auditory neurons in the owl. *Science* **198,** 1278–1280 (1977).
4. Sakitt, B. Indices of discriminability. *Nature* **241,** 133–134 (1973).
5. Sokolov, E. N. Higher nervous functions: the orienting reflex. *Annu. Rev. Physiol.* **25,** 545–580 (1963).
6. Keller, C. H., Hartung, K. & Takahashi, T. T. Head-related transfer functions of the barn owl: measurement and neural responses. *Hear. Res.* **118,** 13–34 (1998).
7. Hall, J. L. Binaural interaction in the accessory superior-olivary nucleus of the cat. *J. Acoust. Soc. Am.* **37,** 813–823 (1965).
8. Baldi, P. & Heiligenberg, W. How sensory maps could enhance resolution through ordered arrangements of broadly tuned receivers. *Biol. Cybern.* **59,** 313–318 (1988).
9. Eurich, C. & Swegler, H. Coarse coding: calculation of the resolution achieved by a population of large receptive field neurons. *Biol. Cybern.* **76,** 357–363 (1997).
10. Fitzpatrick, D. C., Batra, R., Stanford, T. R., Kuwada, S. A neuronal population code for sound localization. *Nature* **388,** 871–874 (1997).
11. Barlow, H. B. Single units and sensation: a neuron doctrine for perceptual psychology? *Perception* **1,** 371–394 (1972).
12. Shackleton, T. M., Skottun, B. C., Arnott, R. H. & Palmer, A. R. Interaural time difference discrimination thresholds for single neurons in the inferior colliculus of guinea pigs. *J. Neurosci.* **23,** 716–724 (2003).
13. Georgopoulos, A. P., Schwartz, A. B. & Kettner, R. E. Neuronal population coding of movement direction. *Science* **233,** 1416–1419 (1986).
14. Newsome, W. T., Britten, K. H. & Movshon, J. A. Neuronal correlates of a perceptual decision. *Nature* **341,** 52–54 (1989).
15. Britten, K. H., Shadlen, M. N., Newsome, W. T. & Movshon, J. A. The analysis of visual motion: a comparison of neuronal and psychophysical performance. *J. Neurosci.* **12,** 4745–4765 (1992).
16. Shadlen, M. N., Britten, K. H., Newsome, W. T. & Movshon, J. A. A computational analysis of the relationship between neuronal and behavioral responses to visual motion. *J. Neurosci.* **16,** 1486–1510 (1996).
17. Recanzone, G. H., Guard, D. C., Phan, M. L. & Su, T. I. Correlation between the activity of single auditory cortical neurons and sound-localization behavior in the macaque monkey. *J. Neurophysiol.* **83,** 2723–2739 (2000).
18. Rolls, E. T., Sienkiewicz, Z. J. & Yaxley, S. Hunger modulates the responses to gustatory stimuli of single neurons in the caudolateral orbitofrontal cortex of the macaque monkey. *Eur. J. Neurosci.* **1,** 53–60 (1989).
19. Farel, P. B. & Thompson, R. F. Habituation of a monosynaptic response in frog spinal cord: evidence for a presynaptic mechanism. *J. Neurophysiol.* **39,** 661–666 (1976).
20. Kandel, E. R., Brunelli, M., Byrne, J. & Castellucci, V. A common presynaptic locus for the synaptic changes underlying short-term habituation and sensitization of the gill-withdrawal reflex in aplysia. *Cold Spring Harb. Symp. Quant. Biol.* **40,** 465–482 (1976).
21. Britten, K. H. & Heuer, H. W. Spatial summation in the receptive fields of MT neurons. *J. Neurosci.* **19,** 5074–5084 (1999).
22. Rolls, E. T. & Treves, A. *Neural Networks and Brain Function* (Oxford Univ. Press, Oxford, 1998).
23. O'Reilly, R. C. & Norman, K. A. Hippocampal and neocortical contributions to memory: advances in the complementary learning systems framework. *Trends Cogn. Sci.* **6,** 505–510 (2002).
24. Siebert, W. M. in *Recognizing Patterns* (eds Kolers, P. A. & Eden, M.) 104–133 (MIT Press, Cambridge, MA, 1968).
25. Colburn, H. S. Theory of binaural interaction based on auditory-nerve data. I. General strategy and preliminary results on interaural discrimination. *J. Acoust. Soc. Am.* **54,** 1458–1470 (1973).
26. Ahissar, M., Ahissar, E., Bergman, H. & Vaadia, E. Encoding of sound-source location and movement: activity of single neurons and interactions between adjacent neurons in the monkey auditory cortex. *J. Neurophysiol.* **67,** 203–215 (1992).
27. Fujita, I. & Konishi, M. The role of GABAergic inhibition in processing of interaural time difference in the owl's auditory system. *J. Neurosci.* **11,** 722–739 (1991).
28. Zohary, E., Shadlen, M. N. & Newsome, W. T. Correlated neuronal discharge rate and its implications for psychophysical performance. *Nature* **370,** 140–143 (1994).
29. Bell, C. C. Memory-based expectations in electrosensory systems. *Curr. Opin. Neurobiol.* **11,** 481–487 (2001).
30. Gold, J. I. & Shadlen, M. N. Representation of a perceptual decision in developing oculomotor commands. *Nature* **404,** 390–394 (2000).

Acknowledgements We thank K. Keller for technical assistance, and J. Bala, S. Colburn, P. Dassonville and R. Marrocco for comments on the manuscript. This work was supported by grants from the National Institute on Deafness and Other Communication Disorders and the McKnight Foundation to T.T.T., and from the NIH to M.W.S.

Competing interests statement The authors declare that they have no competing financial interests.

Correspondence and requests for materials should be addressed to A.B. (avinash@uoneuro.uoregon.edu).